

Instantaneous Spin Correlations in La_2CuO_4

R. J. Birgeneau, M. Greven¹, M. A. Kastner, Y. S. Lee, and B. O. Wells²
Department of Physics, Massachusetts Institute of Technology, Cambridge, MA 02139, USA

Y. Endoh and K. Yamada³
Department of Physics, Tohoku University, Aramaki, Aoba-ku, Sendai 980, 980-77 Japan

G. Shirane
Brookhaven National Laboratory, Upton, NY 11973, USA
 (July 8, 2021)

We have carried out a neutron scattering study of the instantaneous spin-spin correlations in La_2CuO_4 ($T_N = 325$ K) over the temperature range 337 K to 824 K. Incident neutron energies varying from 14.7 meV to 115 meV have been employed in order to guarantee that the energy integration is carried out properly. The results so-obtained for the spin correlation length as a function of temperature when expressed in reduced units agree quantitatively both with previous results for the two dimensional (2D) tetragonal material $\text{Sr}_2\text{CuO}_2\text{Cl}_2$ and with quantum Monte Carlo results for the nearest neighbor square lattice $S=1/2$ Heisenberg model. All of the experimental and numerical results for the correlation length are well described without any adjustable parameters by the behavior predicted for the quantum non-linear sigma model in the low temperature renormalized classical regime. The amplitude, on the other hand, deviates subtly from the predicted low temperature behavior. These results are discussed in the context of recent theory for the 2D quantum Heisenberg model.

PACS numbers: 75.10.Jm, 75.50.Ee, 75.40.Cx, 64.60.Kw

The physics of low dimensional quantum Heisenberg antiferromagnets has been the subject of research ever since the advent of modern quantum and statistical mechanics [1,2]. Interest in two dimensional (2D) systems was heightened by the discovery of high temperature superconductivity in the lamellar copper oxides [3]. Specifically, it was realized early on that the parent compounds such as La_2CuO_4 correspond to rather good approximations to the $S=1/2$ 2D square-lattice quantum Heisenberg antiferromagnet (2DSLQHA)[4,5]. It seems at least possible that the 2D magnetism may in some way be essential to the superconductivity in the charge carrier doped cuprates. Further, the magnetism itself is of fundamental interest as a quantum many body phenomenon in lower dimensions.

Early experiments by Endoh and co-workers [5] showed that over a wide range of temperatures above the three dimensional Néel ordering transition in $\text{La}_2\text{CuO}_{4+y}$ (that is, La_2CuO_4 with a small amount of excess oxygen) the instantaneous spin-spin correlations were purely two dimensional and that the correlation length diverged exponentially in $1/T$. This led to a flurry of theoretical activity [2] including most especially work based on the quantum non-linear sigma model (QNL σ M) by Chakravarty, Halperin and Nelson (CHN) [6] and Hasenfratz and Niedermayer (HN) [7]. These theories are all based on the 2D Heisenberg Hamiltonian which for nearest neighbor (nn) interactions alone takes the form

$$H = J \sum_{\langle i, \delta_{nn} \rangle} \vec{S}_i \cdot \vec{S}_{i+\delta_{nn}} \quad (1)$$

where the summation is over nn pairs on a square lattice.

In La_2CuO_4 , for temperatures below the tetragonal ($I4/mmm$) - orthorhombic ($Bmab$) structural phase transition temperature of $T_{st} = 530$ K, the leading terms in the spin Hamiltonian [8,9] are

$$\begin{aligned} H = J (& \sum_{\langle i, \delta_{nn} \rangle} \vec{S}_i \cdot \vec{S}_{i+\delta_{nn}} + \alpha_{nnn} \sum_{\langle i, \delta_{nnn} \rangle} \vec{S}_i \cdot \vec{S}_{i+\delta_{nnn}} \\ & + \alpha_{xy} \sum_{\langle i, \delta_{nn} \rangle} S_i^c S_{i+\delta_{nn}}^c + \sum_{\langle i, \delta_{\perp j} \rangle} \alpha_{\perp j} \vec{S}_i \cdot \vec{S}_{i+\delta_{\perp j}} \\ & + \alpha_{DM} \sum_{\langle i, \delta_{nn} \rangle} (-)^i \hat{a} \cdot \vec{S}_i \times \vec{S}_{i+\delta_{nn}}). \end{aligned} \quad (2)$$

Here, α_{nnn} , α_{xy} , $\alpha_{\perp j}$, and α_{DM} represent the reduced next nearest neighbor in-plane Heisenberg exchange coupling, XY anisotropy, interlayer coupling and Dzyaloshinski-Moriya antisymmetric exchange, respectively, and S_i^c is the c component of the spin at site i . The fourth term in Eq. (2) explicitly includes the two different out-of-plane neighbors at $\delta_{\perp 1}$ and $\delta_{\perp 2}$. Note that, as was implicit in the work of Thio *et al.* [8], the sign of the antisymmetric term changes on opposite sublattices because of the opposite rotation of the CuO_6 octahedra. This Dzyaloshinski-Moriya term originates from a small rotation of the CuO_6 octahedra about the \hat{a} axis. In the tetragonal phase $\alpha_{DM} = 0$ and the nearest neighbor out-of-plane effective coupling vanishes since $\alpha_{\perp 1} = \alpha_{\perp 2}$.

The most complete experimental study to-date is on the material $\text{Sr}_2\text{CuO}_2\text{Cl}_2$ [10] rather than La_2CuO_4 . The reasons for this are twofold: First, $\text{Sr}_2\text{CuO}_2\text{Cl}_2$ is very

difficult to dope so that there are no complications arising from the effects of doped electrons or holes on the spin correlations. Second, since $\text{Sr}_2\text{CuO}_2\text{Cl}_2$ is tetragonal down to the lowest temperatures measured (< 10 K), $\alpha_{DM}=0$ and the nearest neighbor interplanar coupling vanishes to leading order, that is $\alpha_{\perp 1} = \alpha_{\perp 2}$. As shown in Table (1) there is a small XY anisotropy. In addition, from results in $\text{Sr}_2\text{Cu}_3\text{O}_4\text{Cl}_2$ [11], we infer that there is a next nearest neighbor in-plane Heisenberg exchange coupling which is about 8% of the nearest neighbor value. To first order, the latter should simply lead to a slight renormalization of the effective J in Eq. (1). The XY anisotropy will lead to a crossover from Heisenberg to XY behavior for correlation lengths $\xi/a \gtrsim 100$. Thus, $\text{Sr}_2\text{CuO}_2\text{Cl}_2$ should be a good realization of the S=1/2 2DSLQHA for length scales $\lesssim 100$. This has, in fact, been confirmed in detail experimentally [10]; specifically, over a wide range of length scales the 2D correlation length measured in $\text{Sr}_2\text{CuO}_2\text{Cl}_2$ agrees quantitatively with results from quantum Monte Carlo (QMC) calculations carried out on the Hamiltonian Eq. (1) with S=1/2 [12-14]. The value for J for $\text{Sr}_2\text{CuO}_2\text{Cl}_2$ listed in Table (1) is deduced from two magnon Raman scattering measurements [15].

Both the QMC and the $\text{Sr}_2\text{CuO}_2\text{Cl}_2$ experimental results for the correlation length in turn are quantitatively predicted by theory based on the QNL σ M in the low temperature renormalized classical (RC) regime [6, 7]. This comparison again involves no adjustable parameters. Surprisingly, this agreement holds for correlation lengths as short as a few lattice constants. This is far outside of the temperature range where the QNL σ M-RC theory should hold. A plausible explanation for this unexpected agreement has been given by Beard *et al.*[13]

In spite of the fact that the progenitor of this work was the discovery of high temperature superconductivity in $\text{La}_{2-x}\text{Ba}_x\text{CuO}_4$ [3] together with the early work on the 2D spin correlations in $\text{La}_2\text{CuO}_{4+y}$ [5], our

	La_2CuO_4	$\text{Sr}_2\text{CuO}_2\text{Cl}_2$
S	1/2	1/2
T_N (K)	325	256.5
J (meV)	135	125
α_{nnn}	~ 0.08	~ 0.08
α_{DM}	1.5×10^{-2}	-
α_{XY}	-5.7×10^{-4}	-5.3×10^{-4}
$\alpha_{\perp 1} - \alpha_{\perp 2}$	5×10^{-5}	$\sim 10^{-8}$

TABLE I. Néel temperature, superexchange energy, and corrections to the 2D Heisenberg Hamiltonian for La_2CuO_4 [9] and $\text{Sr}_2\text{CuO}_2\text{Cl}_2$ [10]. α_{DM} and α_{XY} are larger than the values quoted in references [9] and [10] by factors of (Z_c/Z_g) and $(Z_c/Z_g)^2$ respectively. Here $Z_c(1/2) \simeq 1.17$ and $Z_g(1/2) \simeq 0.6$ are the quantum renormalization factors for the spin wave velocity and spin wave gap respectively.

knowledge of the spin correlations in stoichiometric La_2CuO_4 is rather limited. The primary correlation length data for La_2CuO_4 originate from the neutron scattering study of Keimer *et al.* [9] on a carrier-free single crystal of La_2CuO_4 with $T_N = 325$ K. The Keimer *et al.* [9] data on the correlation length and structure factor extend up to 550 K. Their measurements are generally consistent with the $\text{Sr}_2\text{CuO}_2\text{Cl}_2$, QMC and QNL σ M-RC results, but there appear to be systematic discrepancies at the limit of the error bars for the correlation length at both low and high temperatures. These neutron experiments were carried out using a single incident neutron energy of 31 meV. It seems likely that the discrepancies are an experimental artifact originating from the use of a single incident neutron energy over a wide range of temperatures. Alternatively, they could represent a real effect originating from the antisymmetric exchange and interplanar coupling terms in Eq. (2) for La_2CuO_4 . Clearly, therefore, it is important to carry out a more complete study of the spin-spin correlations in La_2CuO_4 in order to characterize fully the magnetism in this parent compound of the monolayer high temperature superconductors. Such data would also be valuable for the interpretation of NQR results in La_2CuO_4 [16]. Finally, there have been some important advances in our understanding of the theory for the 2DSLQHA since the work of Greven *et al.*[10] on $\text{Sr}_2\text{CuO}_2\text{Cl}_2$ and it is therefore of value to re-examine the relationships between the results of experiments in real systems and theory.

The experiments were carried out primarily on the H7 triple-axis spectrometer at the High Flux Beam Reactor at Brookhaven National Laboratory. The measurements utilized the same single crystal of La_2CuO_4 as employed by Keimer *et al.* [9]; this crystal had a volume of about 1.5 cm^3 . Throughout this paper we use $Bmab$ orthorhombic axes; at $T_N = 325$ K the lattice constants are $a = 5.338 \text{ \AA}$, $b = 5.406 \text{ \AA}$, and $c = 13.141 \text{ \AA}$. We show in Fig. 1 the temperature dependence of the (0 1 2) nuclear superlattice peak intensity together with the reduced orthorhombic splitting $(b-a)/(b+a)$ [17]. As is evident from Fig. 1, the sample of La_2CuO_4 shows a sharp tetragonal-orthorhombic structural phase transition at $T_{st} = 530.5 \pm 0.5$ K. The sharpness of the transition in turn reflects the microscopic homogeneity of this sample.

The magnetic neutron scattering experiments were carried out in the energy-integrating two axis mode. For 2D systems the integration over energy is carried out automatically in a two axis experiment provided that the outgoing neutron wave vector \vec{k}_f is perpendicular to the 2D planes and provided that the neutron energy is significantly larger than the characteristic energy ω_0 of the spin fluctuations at a given temperature [18]. From the theory of CHN [6, 19] one has

$$\omega_0^{CHN} = \frac{c}{\xi} \left(\frac{T}{2\pi\rho_s} \right)^{1/2} \quad (3)$$

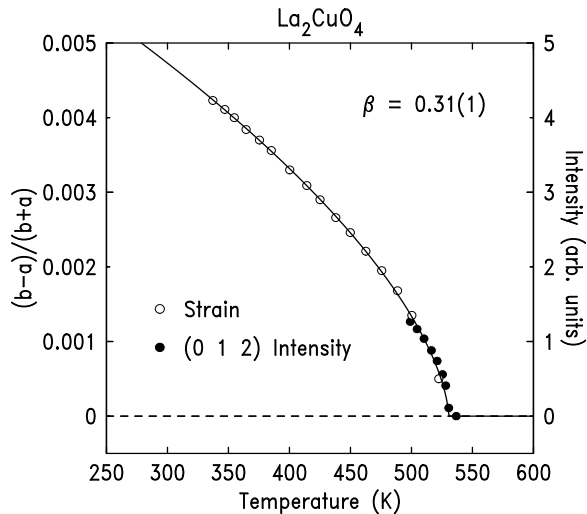


FIG. 1. Orthorhombic splitting and (0,1,2) superlattice peak intensity versus temperature; the data are normalized relative to each other in the temperature region of overlap. The solid line is the result of a fit to a power law $A(T_{st}-T)^{2\beta}$ with $\beta = 0.31 \pm 0.01$ and $T_{st} = 530.5 \pm 0.5$ K.

where c and ρ_s are the zero temperature spin wave velocity and spin stiffness respectively. For La_2CuO_4 this becomes [20]

$$\omega_0^{CHN} \simeq \frac{850 \text{ meV}\text{\AA}}{\xi} \sqrt{\frac{T}{1800}} \quad (4)$$

Quantum Monte Carlo calculations by Makivić and Jarrell [21] at intermediate temperatures generally are well described by Eq. (4) but with an amplitude that is approximately twice as large. Specifically, Makivić and Jarrell [21] find that between 550 K and 800 K for $J = 135$ meV, as in La_2CuO_4 [20], ω_0 varies from ~ 25 meV to ~ 63 meV. Accordingly, the following protocol was used in our measurements. Neutrons with incident energies $E_i = 14.7$ meV were used at the lower temperatures. With increasing temperature and hence decreasing ξ the incoming neutron energy was progressively raised to 41 meV, 90 meV and 115 meV. To ensure that the energy integration was carried out correctly, it was required that the results for the correlation length in the temperature regions of overlap agreed with each other to well within the experimental errors.

We show first in Fig. 2 preparatory data taken at a temperature of $T = 328$ K which is just above the 3D Néel temperature of 325 K. The incident neutron energy was $E_i = 3.6$ meV which results in very high momentum resolution. The two peaks evident in Fig. 2 originate from the two rods of scattering which are along $(1,0,l)$ and $(0,1,l)$, respectively. The equi-intensity of the two peaks implies that at 328 K the 2D spin fluctuations have at least XY symmetry, that is, at 328 K there is no measurable in-plane anisotropy induced by the antisymmetric exchange terms in Eq. (2).

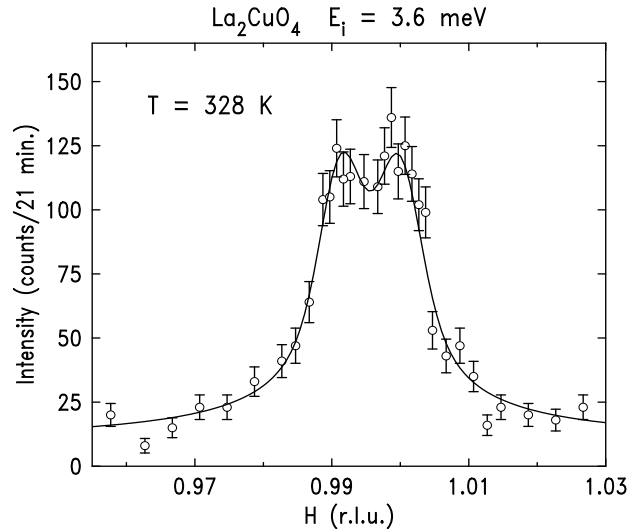


FIG. 2. $E = 3.6$ meV two-axis scan across the 2D rods at $(1,0,1.59)$ and $(0,1,1.59)$. The solid line is the result of a fit to two Lorentzians, Eq. (5), centered about $(1,0,l)$ and $(0,1,l)$ respectively, convolved with the instrumental resolution function. The fit gives $\xi^{-1} = 0.0011 \pm 0.0004$ reciprocal lattice units.

In Figs. 3 and 4 some representative energy-integrating scans for $E_i = 41$ meV and $E_i = 115$ meV are shown. The collimations were set to $20' - 10' - S - 10'$ in both cases, and for neutrons with $E_i = 41$ meV a pyrolytic graphite filter was used. For $E_i = 115$ meV, the experiment was carried out without a filter in order to maximize the neutron flux. Higher order contamination from neutrons with energies above ~ 400 meV is not a concern as it results from the high-energy-tail of the thermal neutron spectrum peaked at ~ 30 meV. The solid lines in Figs. 3 and 4 are the result of fits to the 2D Lorentzian form

$$\mathcal{S}(\vec{q}_{2D}) = \frac{\mathcal{S}(0)}{1 + q_{2D}^2 \xi^2}, \quad (5)$$

where \vec{q}_{2D} is the 2D deviation in wave vector from the positions of the $(1,0,l)$ and $(0,1,l)$ rods, convolved with the instrumental resolution function of the spectrometer.

The results so-obtained for the inverse correlation length ξ^{-1} are shown in Fig. 5. These data are consistent within the errors with the earlier results of Keimer *et al.* [9], but are much more precise and cover a wider range of temperatures. The solid line is the predicted behavior for the QNL σ M in the renormalized classical regime [6, 7]; this will be discussed below. The results for the Lorentzian amplitude $\mathcal{S}(0)/\xi^2$ are shown in Fig. 6. The four sets of data are normalized to unity over the temperature interval $450 \text{ K} \leq T \leq 550 \text{ K}$.

We now compare the results in Fig. 5 for the correlation length in La_2CuO_4 with the predictions of various theories. We begin with the results of QMC calculations

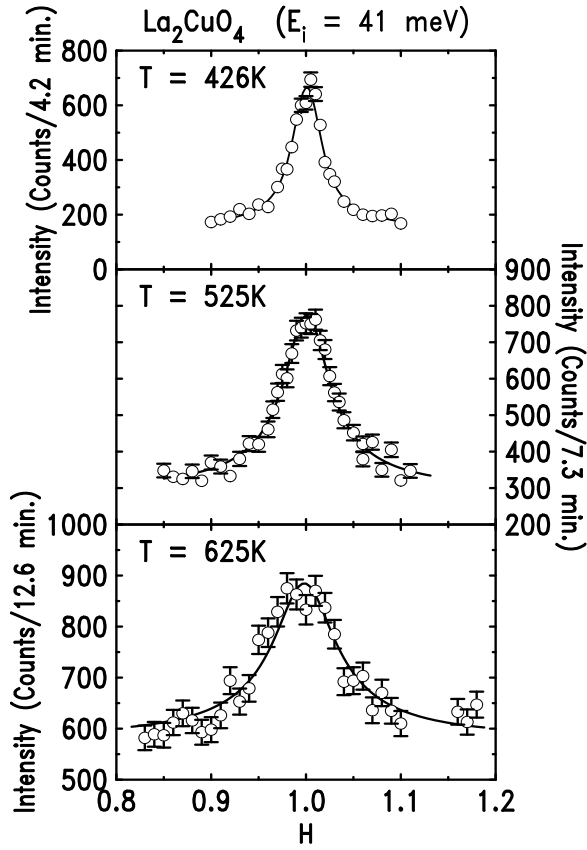


FIG. 3. Representative energy-integrating two-axis scans in La_2CuO_4 with $E_i = 41$ meV and collimations $20' - 10' - S - 10'$. The solid lines are the result of fits to a 2D Lorentzian scattering function Eq. (5) convolved with the resolution function of the spectrometer.

for Eq. (1) with $S = 1/2$. Because of both advances in computational techniques and the implementation of finite-size scaling methods, QMC data now exist for ξ/a for the $S = 1/2$ nn 2DSLQHA for length scales varying from 1 to 350,000 lattice constants. QMC results of Beard *et al.* [13] and Kim and Troyer [14] are plotted in Fig. 7 together with our experimental results in La_2CuO_4 . The data are plotted in the reduced form ξ/a vs. J/T . It is evident that the QMC and La_2CuO_4 results agree in absolute units over the complete temperature range ($337 \text{ K} < T < 824 \text{ K}$) or equivalently, length scale range ($3 \lesssim \xi/a \lesssim 115$). Thus, over this range the 2D spin correlations in La_2CuO_4 are entirely determined by the leading near-neighbor Heisenberg couplings and the anisotropic in-plane plus interplanar terms in Eq. (2) have no measurable effect to within the uncertainty of our experiments. Specifically, the tetragonal-orthorhombic structural phase transition at 530 K does not manifest itself in the temperature dependence of the correlation length.

We now consider the predictions of various analytical theories. A low-temperature theory for the 2DSLQHA

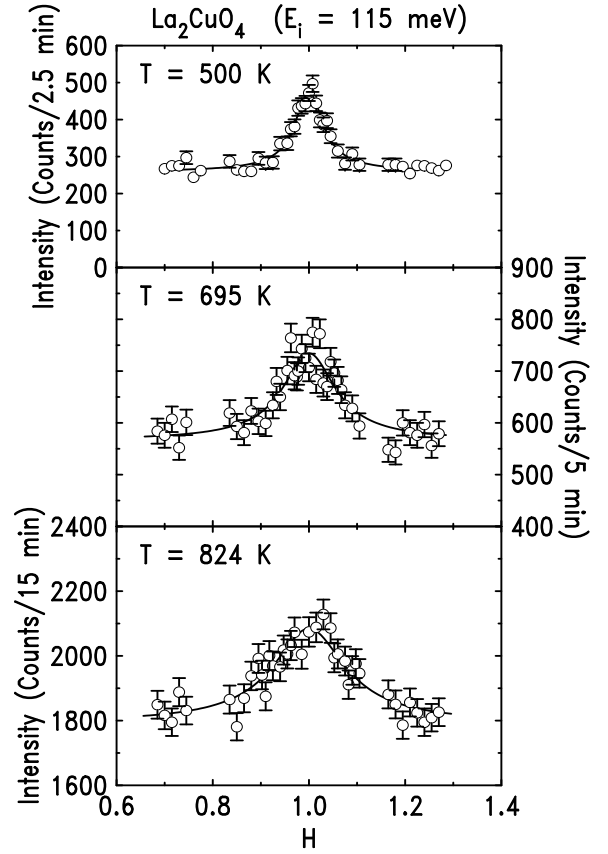


FIG. 4. Representative energy-integrating two-axis scans in La_2CuO_4 with $E_i = 115$ meV and collimations $20' - 10' - S - 10'$. The solid lines are the results of fits to a 2D Lorentzian scattering function convolved with the resolution function of the spectrometer.

was formulated by Chakravarty, Halperin, and Nelson [6], in which they obtained the static and dynamic properties of the 2DSLQHA by mapping it onto the 2D quantum non-linear σ model. The 2D QNL σ M is the simplest continuum model which reproduces the correct spin-wave spectrum and spin-wave interactions of the 2DSLQHA at long wavelengths and low energies. First, CHN argued that for $S \geq 1/2$ the nn 2DSLQHA corresponds to the region of the 2D QNL σ M in which the ground state is ordered - the renormalized classical regime. Then, CHN used perturbative renormalization group arguments to derive an expression for the correlation length to two-loop order, showing a leading exponential divergence of ξ versus inverse temperature. Later, Hasenfratz and Niedermayer [7] employed chiral perturbation theory to calculate the correlation length more precisely to three-loop order. In the RC scaling regime, the correlation length is given by

$$\frac{\xi}{a} = \frac{e}{8} \frac{c/a}{2\pi\rho_s} e^{2\pi\rho_s/T} \left[1 - \frac{1}{2} \left(\frac{T}{2\pi\rho_s} \right) + \mathcal{O} \left(\frac{T}{2\pi\rho_s} \right)^2 \right], \quad (6)$$

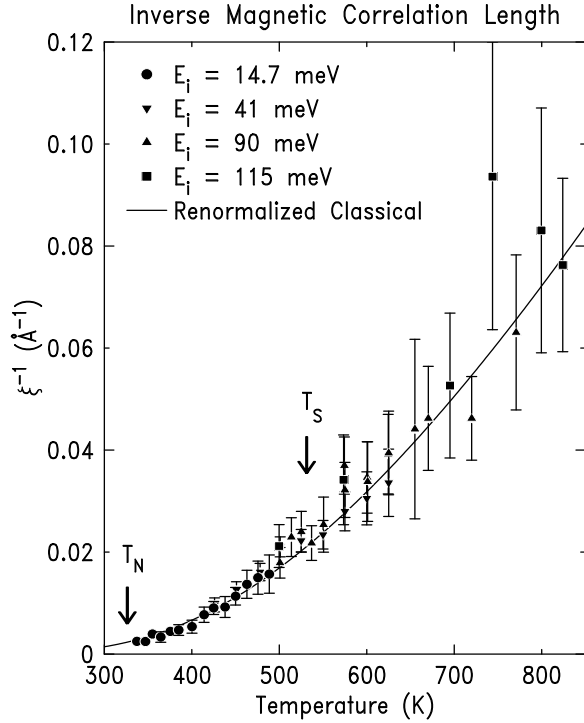


FIG. 5. Inverse magnetic correlation length of La_2CuO_4 . The solid line is Eq. (6) with $J = 135$ meV. The Néel and structural transition temperatures are indicated by arrows.

which we refer to as the CHN-HN formula. The parameters ρ_s and c are the macroscopic $T = 0$ spin stiffness and spin-wave velocity, respectively. For the nearest-neighbor 2DSLQHA, they are related to the microscopic parameters J, S and the lattice constant a according to $\rho_s = Z_\rho(S)S^2J$ and $c = Z_c(S)2\sqrt{2}aSJ$. The coefficients $Z_\rho(S)$ and $Z_c(S)$ are quantum renormalization factors, which can be calculated using spin-wave theory ($S \geq 1/2$) [22, 23], series expansion ($S = 1/2, 1$) [23], and Monte Carlo techniques ($S = 1/2$) [12-14]. For $S = 1/2$, the spin-wave approximation gives $Z_\rho(1/2) \simeq 0.699$ and $Z_c(1/2) \simeq 1.18$ [22, 23]. The most precise values for $S = 1/2$ currently available come from the QMC study of Beard *et al.* [13] who find $c = 1.657(2)Ja$, and $\rho_s = 0.1800(5)J$ and, for the $T=0$ sublattice magnetization, $M_s = 0.30797(3)/a^2$. These correspond to $Z_c(1/2) = 1.172$ and $Z_{\rho_s}(1/2) = 0.72$. The CHN-HN prediction for the Lorentzian amplitude $S(0)/\xi^2$ is

$$\frac{S(0)}{\xi^2} = A2\pi M_s^2 \left(\frac{T}{2\pi\rho_s} \right)^2 \left[1 + C_1 \frac{T}{2\pi\rho_s} + \mathcal{O} \left(\frac{T}{2\pi\rho_s} \right)^2 \right], \quad (7)$$

It is of interest to compare the QNL σ M predictions with the corresponding predictions of the classical spin model for the *nn* 2DSLHA at low temperatures [2,6,24,25]

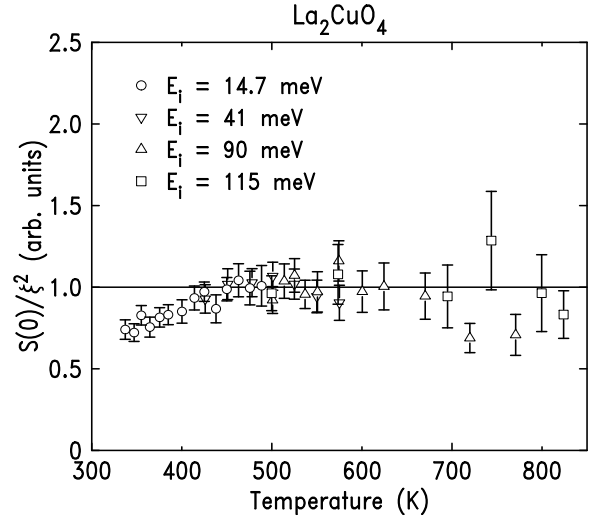


FIG. 6. Lorentzian amplitude, $S(0)/\xi^2$ versus temperature. The data for the different incident neutron energies are normalized to unity in the temperature range $450 \text{ K} \lesssim T \lesssim 550 \text{ K}$.

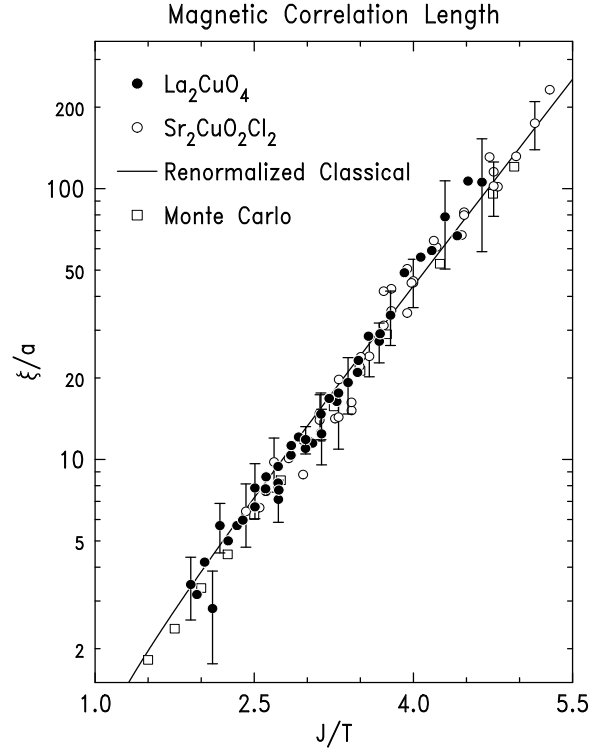


FIG. 7. The logarithm of the reduced magnetic correlation length ξ/a versus J/T . The closed circles are data for La_2CuO_4 plotted with $J = 135$ meV, the open circles are data for $\text{Sr}_2\text{CuO}_2\text{Cl}_2$ plotted with $J = 125$ meV [10], and the open squares are the results of the Monte Carlo computer simulations [12-14]. The solid line is the theoretical prediction without adjustable parameters of the 2DQNL σ M for the renormalized classical regime Eq. (6).

$$\frac{\xi}{a} = 0.0125 \frac{T}{2\pi\rho_{cl}} e^{2\pi\rho_{cl}/T} \left[1 - b_1 \frac{T}{2\pi\rho_{cl}} + \mathcal{O}\left(\frac{T}{\rho_{cl}}\right)^2 \right] \quad (8)$$

and

$$\frac{\mathcal{S}(0)}{\xi^2} = A2\pi M_s^2 \left(\frac{T}{2\pi\rho_{cl}}\right)^2 \left[1 + C_1 \frac{T}{2\pi\rho_{cl}} + \mathcal{O}\left(\frac{T}{\rho_{cl}}\right)^2 \right] \quad (9)$$

where for classical unit vector spins, $\rho_{cl} = J$. For large S quantum spins, one finds that the classical limit is approached smoothly as a function of S provided that temperature is measured in units of $JS(S+1)$, implying one that should take $\rho_{cl} = JS(S+1)$ [2]. This choice for $S = 1/2$, gives $\rho_{cl} = 0.75J$ compared with $\rho_s = 0.18J$. The arguments in the exponentials in Eq. (6) and (8) then differ by more than a factor of 4 – a very dramatic difference between renormalized classical and classical scaling behavior.

An alternative theoretical analysis of the 2DSLQHA has been carried out by Cuccoli *et al.* [26] in which they treat quantum fluctuations in a self-consistent Gaussian approximation separately from the classical contribution. In their approach, which they label the purely-quantum self-consistent harmonic approximation (PQSCHA), the quantum spin Hamiltonian is rewritten as an effective classical Hamiltonian, where the temperature scale is renormalized due to quantum fluctuations, and the new classical spin length appears as $S + 1/2$. Defining the reduced temperature as $t = T/\{J(S + 1/2)^2\}$, the correlation length for the 2DSLQHA is then simply given by

$$\xi(t) = \xi_{cl}(t_{cl}) \quad \text{with} \quad t_{cl} = \frac{t}{\theta^4(t)}. \quad (10)$$

Here, ξ_{cl} is the correlation length for the corresponding classical 2D square-lattice nn Heisenberg model, which is given by Eq. (8) at low temperatures and may be obtained from classical spin Monte Carlo calculations at higher temperatures [27], and $\theta^4(t)$ is a temperature renormalization parameter. The PQSCHA is most accurate in the limit where the quantum fluctuations are weak, and correspondingly θ^4 is near unity. This is the case for large spin, for example, $S=5/2$, and indeed this has recently been studied experimentally by Leheny *et al.* [28] who have measured $\mathcal{S}(\vec{q}_{2D})$ in the $S = 5/2$ 2DSLQHA material Rb_2MnF_4 . They follow a field-temperature trajectory which approaches the bicritical point in the phase diagram and which accordingly should show pure 2D Heisenberg behavior. In this case the PQSCHA predicts the correlation length precisely with no adjustable parameters over the inverse temperature range $0.5 < \rho_{cl}/T < 2$ or equivalently, the length

scale range $1 < \xi/a \lesssim 100$. We note from Eq. (8) and (9) that for the classical model T always appears scaled by ρ_{cl} . Thus the quantum effects in the PQSCHA can be thought of simply as a temperature dependent renormalization of ρ_{cl} , that is, $\rho_{cl} \rightarrow \theta^4(t)\rho_{cl}$.

Finally, for the QNL σ M there may be a crossover from renormalized classical to quantum critical behavior with increasing temperature [6]. In the QC regime heuristically one expects

$$\xi/a = 0.8 \frac{c/a}{T - T_{QC}} \quad (11)$$

with $T_{QC} \geq 0$ adjustable [2,6,10]. We emphasize that this anticipated crossover is a property of the QNL σ M and it may or may not occur for quantum spins on a 2D lattice.

The solid line in Fig. 5 is the QNL σ M-RC prediction, Eq. (6) with c and ρ_s from Beard *et al.* [13] As observed previously for $\text{Sr}_2\text{CuO}_2\text{Cl}_2$ [10], Eq. (6) describes the measured correlation length of La_2CuO_4 extremely well without adjustable parameters over the temperature range $337 \text{ K} < T < 824 \text{ K}$, or equivalently, the length scale range, $\sim 3 \lesssim \xi/a \lesssim 110$. All of the data for ξ/a from each of quantum Monte Carlo, $\text{Sr}_2\text{CuO}_2\text{Cl}_2$ and La_2CuO_4 together with Eq. (6) are plotted in the universal form ξ/a vs. J/T in Fig. 7. The evident universal behavior is, of course, both pleasing and reassuring. The good agreement of all of the experimental and numerical results with the low temperature QNL σ M-RC predictions down to very small values of J/T at first appears to be quite puzzling. The QMC study, Ref. [13], suggests that this agreement is, at least in part, accidental. Specifically, in crossing over from the low temperature continuum QNL σ M to the discrete lattice $S=1/2$ Heisenberg model the higher order terms in Eq. (6) conspire such that over the measured temperature range the deviation of ξ/a from Eq. (6) is never more than 15% which is well within the experimental error.

We now focus on the high temperature behavior in La_2CuO_4 . We show in Fig. 8 the La_2CuO_4 correlation length data together with the predictions from QNL σ M-RC (Eq. (6)), QNL σ M-QC Eq. (11), high temperature series expansion [29] and the PQSCHA which involves Eq. (10) combined with results of classical Monte Carlo simulations [27]. As observed previously for $\text{Sr}_2\text{CuO}_2\text{Cl}_2$ [10] as well as for both $S = 1/2$ 2DSLQHA QMC calculations [14] and high temperature series expansion results [29], the QNL σ M-QC prediction, Eq. (11), disagrees strongly with the experimental results in La_2CuO_4 . This is, perhaps, not surprising given the extremely short length scales at the relevant temperatures. Specifically, at these short distances, the continuum QNL σ M approach which underlies the possible QC behavior is probably no longer valid. By contrast the PQSCHA which corresponds to classical scaling for the pure 2D

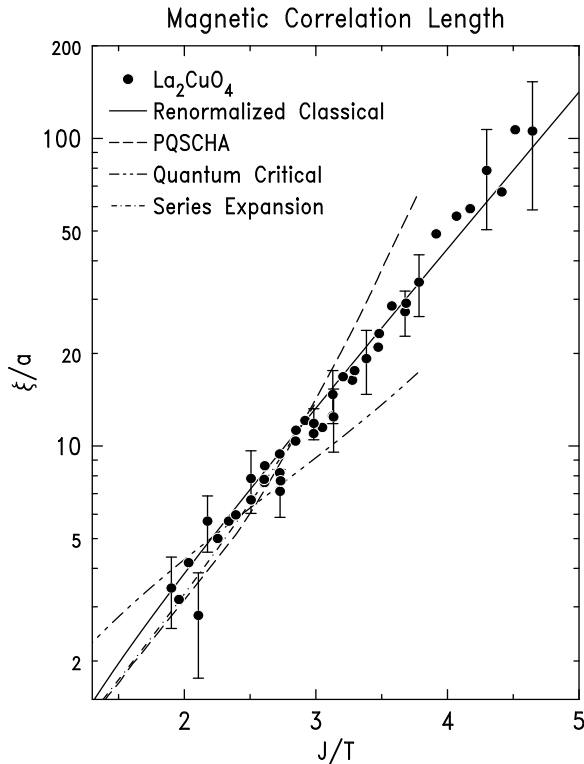


FIG. 8. The logarithm of the reduced magnetic correlation length ξ/a versus J/T compared with the predictions of various theories including renormalized classical behavior, Eq. (6), quantum critical behavior, Eq. (11), the PQSCHA, Eq. (10), and high temperature series expansion [29].

Heisenberg model [2,30] agrees reasonably well in absolute units with no adjustable parameters for length scales up to about $\xi/a \sim 15$. As expected, the PQSCHA breaks down at lower temperatures and larger length scales. Thus, if there is a crossover in the correlation length, it is from classical scaling to renormalized classical scaling with decreasing temperature. Clearly, it is very important that theory for this crossover from the high temperature PQSCHA classical scaling regime to the low temperature QNL σ M-RC regime be developed.

Finally, we discuss the behavior of the structure factor $\mathcal{S}(0)$. The leading divergence of $\mathcal{S}(0)$ is determined by ξ^2 . This is confirmed by the results for $\mathcal{S}(0)$ in La_2CuO_4 displayed in Fig. 6 which shows that $\mathcal{S}(0)/\xi^2$ is approximately constant over the complete temperature range. This is equivalent to the statement that for the 2D $S=1/2$ QHA the critical exponent $\eta_2 = 0$. We note that in 3D $\eta_3 \simeq 0.04$, [31] that is, $\mathcal{S}(0) \sim \xi^{1.96}$ whereas for the 1D $S=1/2$ QHA one has the remarkable result that $\mathcal{S}(0) \sim (\ln \xi)^{3/2}$ [32], which implies $\eta_1 = 2$.

The temperature dependent correction factors (c.f. Eq. (7)) beyond the leading ξ^2 divergence are problematic. Specifically, Greven *et al.* [10] find in their measurements in $\text{Sr}_2\text{CuO}_2\text{Cl}_2$ that over the length scale $5 \lesssim \xi/a \lesssim 200$, $\mathcal{S}(0)/\xi^2$ is independent of temperature to within the er-

rors. By contrast, QMC [12-14] and high temperature series expansion [29,30] studies of the $S=1/2$ nn 2DSLQHA find $\mathcal{S}(0)/\xi^2 \sim T^2$ over about the same range of length scales. In the $S = 5/2$ 2DSLQHA material Rb_2MnF_4 , Leheny *et al.* [28] find a clear crossover at $\xi/a \sim 4$ from $\mathcal{S}(0)/\xi^2 \sim T^2$ behavior to a much weaker dependence of $\mathcal{S}(0)/\xi^2$ on T . The data for $\mathcal{S}(0)/\xi^2$ in La_2CuO_4 shown in Fig. 5 are clearly inconsistent with T^2 behavior over the complete temperature range but would allow a gradual crossover as found in Rb_2MnF_4 . This lack of universality in $\mathcal{S}(0)/\xi^2$ seems surprising given the robust universality of the behavior for ξ/a (Fig. 7). Of course, departures from the low temperature QNL σ M-RC behavior may occur at different temperatures for different quantities. It is also possible that the terms in Eq. (2) beyond the nearest neighbor Heisenberg coupling will effect $\mathcal{S}(0)/\xi^2$ more than they effect ξ itself.

In summary, we have carried out a neutron scattering study of the instantaneous spin-spin correlations in La_2CuO_4 ($T_N=325$ K) over the temperature range 337 K to 824 K. Incident neutron energies varying from 14.7 meV to 115 meV have been employed in order to guarantee that the energy integration is carried out properly. The results so-obtained for the spin correlation length as a function of temperature when expressed in reduced units agree quantitatively both with previous results for the 2D tetragonal material $\text{Sr}_2\text{CuO}_2\text{Cl}_2$ and with quantum Monte Carlo results for the nearest neighbor square lattice $S = 1/2$ Heisenberg model. All of the experimental results for the correlation length are well described without any adjustable parameters by the behavior predicted for the quantum non-linear sigma model in the low temperature renormalized classical regime. The structure factor, on the other hand, deviates subtly from the predicted low temperature behavior although the leading ξ^2 behavior is confirmed. The correlation length data at high temperature agree reasonably well with predictions of the PQSCHA which corresponds to classical scaling with quantum corrections for the 2D Heisenberg model. We therefore hypothesize that in La_2CuO_4 there is a gradual crossover from renormalized classical to classical scaling with increasing temperature.

Acknowledgements

We would like to acknowledge helpful discussions and communications on these results with S. Charkravarty, T. Imai, R. Leheny, R.R.P. Singh, V. Tognetti, P. Verucchi, U.-J. Wiese and J. Zinn-Justin. This work was supported in part by a Grant-In-Aid for Scientific Research from the Japanese Ministry of Education, Science, Sports and Culture, by a Grant for the Promotion of Science from the Science and Technology Agency and by CREST. Work at Brookhaven National Laboratory was carried out under Contract No. DE-AC02-98-CH10886, Division of Material Science, U.S. Department of Energy.

The research at MIT was supported by the National Science Foundation under Grant No. DMR97-04532 and by the MRSEC Program of the National Science Foundation under Award No. DMR98-08941.

References

- ¹*Permanent address:* Dept. of Applied Physics and Stanford Synchrotron Radiation Laboratory, Stanford University, Stanford, CA 94305, USA
- ²*Permanent address:* Dept. of Physics, Brookhaven National Laboratory, Upton, NY 11973, USA
- ³*Permanent address:* Institute for Chemical Research, Kyoto University, Uji 611-0011, Japan
1. H. A. Bethe, *Z. Phys.* **71**, 205 (1931).
 2. For reviews see: E. Manousakis, *Rev. Mod. Phys.* **63**, 1 (1991); N. Elstner, *Int. J. Mod. Phys.* **B11** 1753 (1997).
 3. J. G. Bednorz and K. A. Müller, *Z. Phys.* **B64**, 189 (1986).
 4. P. W. Anderson, *Science* **235**, 1196 (1987).
 5. Y. Endoh, K. Yamada, R. J. Birgeneau, D. R. Gabbe, H. P. Jørgensen, M. A. Kastner, C. J. Peters, P. J. Picone, T. R. Thurston, J. M. Tranquada, G. Shirane, Y. Hidaka, M. Oda, Y. Enomoto, M. Suzuki, and T. Murakami, *Phys. Rev.* **B37**, 7443 (1988).
 6. S. Chakravarty, B.I. Halperin, and D.R. Nelson, *Phys. Rev.* **B39**, 2344 (1989). For a detailed discussion of the quantum critical region see also A. Chubukov, S. Sachdev and Y. Ye, *Phys. Rev.* **B49** 2344 (1994).
 7. P. Hasenfratz and F. Niedermayer, *Phys. Lett. B* **268**, 231 (1991).
 8. T. Thio, T. R. Thurston, N. W. Preyer, P. J. Picone, M. A. Kastner, H. P. Jørgensen, D. R. Gabbe, C. Y. Chen, R. J. Birgeneau, and A. Aharony, *Phys. Rev. B* **38**, 905 (1988).
 9. B. Keimer, N. Belk, R. J. Birgeneau, A. Casanholo, C. Y. Chen, M. Greven, M. A. Kastner, A. Aharony, Y. Endoh, R. W. Erwin, and G. Shirane, *Phys. Rev.* **B46**, 14034 (1992).
 10. M. Greven, R. J. Birgeneau, Y. Endoh, M. A. Kastner, M. Matsuda, and G. Shirane, *Z. Phys. B* **96**, 465 (1995).
 11. F. C. Chou, A. Aharony, R. J. Birgeneau, O. Entin-Wohlman, M. Greven, A. B. Harnig, M. A. Kastner, Y.-J. Kim, D. S. Kleinberg, Y. S. Lee, and Q. Zhu, *Phys. Rev. Lett.* **78**, 535 (1998); Y.-J. Kim (private communication).
 12. M. Makivić and H.-Q. Ding, *Phys. Rev.* **B43**, 3562 (1991).
 13. B. Beard, R. J. Birgeneau, M. Greven, and U.-J. Wiese, *Phys. Rev. Lett.* **80**, 1742 (1998).
 14. J.-K. Kim and M. Troyer, *Phys. Rev. Lett.* **80**, 2705 (1998).
 15. Y. Tokura, S. Koshihara, T. Arima, H. Takagi, S. Ishibashi, T. Ido, and S. Uchida, *Phys. Rev.* **B41**, 11657 (1990).
 16. T. Imai, C. P. Schlichter, K. Yoshimura, M. Katoh, and K. Kosuge, *Phys. Rev. Lett.* **71**, 1254 (1993).
 17. R. J. Birgeneau, C. Y. Chen, D. R. Gabbe, H. P. Jørgensen, M. A. Kastner, P. J. Picone, T. Thio, T. R. Thurston, and H. L. Tuller, *Phys. Rev. Lett.* **59**, 1329 (1987).
 18. R. J. Birgeneau, J. Skalyo, Jr., and G. Shirane, *Phys. Rev.* **B3**, 1736 (1971).
 19. S. Tyč, B. I. Halperin, and S. Chakravarty, *Phys. Rev. Lett.* **62**, 835 (1989).
 20. G. Aeppli, S. M. Hayden, H. A. Mook, Z. Fisk, S. W. Cheong, D. Rytz, J. P. Remeika, G. P. Espinosa, and A. S. Cooper, *Phys. Rev. Lett.* **62**, 2052 (1989).
 21. M. Makivić and M. Jarrell, *Phys. Rev. Lett.* **68**, 1770 (1992).
 22. J. Igarashi, *Phys. Rev.* **B46**, 10763 (1992).
 23. R.R.P. Singh, *Phys. Rev.* **B39**, 9760 (1989); C. Hamer, Z. Weihong, and J. Oitmaa, *Phys. Rev. B* **50**, 6877 (1994).
 24. Th. Jolicoeur and J. C. LeGouillou, *Mod. Phys. Lett.* **B5**, 593 (1991).
 25. D. R. Nelson and R. A. Pelcovits, *Phys. Rev.* **B16**, 2191 (1977).
 26. A. Cuccoli, V. Tognetti, R. Vaia, and P. Verrucchi, *Phys. Rev.* **B56**, 14456 (1997).
 27. J.-K. Kim, *Phys. Rev.* **D50**, 4663 (1994).
 28. R. L. Leheny, R. J. Christianson, R. J. Birgeneau, and R. W. Erwin, *Phys. Rev. Lett.* **82**, 418 (1999).
 29. A. Sokol, R.L. Glenister and R.R.P. Singh, *Phys. Rev. Lett.*, **72**, 1549 (1994).
 30. N. Elstner, A. Sokol, R. R. P. Singh, M. Greven, and R.J. Birgeneau, *Phys. Rev. Lett.* **75**, 938 (1995).

31. See for example L.C. LeGuillon and J. Zinn-Justin, Phys. Rev. **B21**, 3976 (1980).
32. O.A. Starykh, A.W. Sandvik, and R.R.P. Singh, Phys. Rev. **B55**, 14953 (1997).